

Evaluation of Cytotoxic Activity *in vitro* of Charantin A Extracted from *Momordica charantia*

Zijun Guo^{1,2†}, Guocai Wang^{3†}, Maoxin Zhang⁴, Guangwen Liang⁴,
Qiang Li^{1,2} and Bing Ling^{4*}

¹College of Plant Protection, Yunnan Agricultural University, Kunming 650201, P. R. China

²State Key Laboratory for Conservation and Utilization of Bio-Resources in Yunnan, Yunnan Agricultural University, Kunming 650201, P. R. China

³Institute of Traditional Chinese Medicine and Natural Products, College of Pharmacy, Jinan University, Guangzhou 510632, P. R. China

⁴Key Laboratory of Bio-Pesticide Innovation and Application of Guangdong Province, College of Agriculture, South China Agricultural University, Guangzhou 510640, P. R. China

(Received December 04, 2017; Revised March 01, 2018; Accepted March 02, 2018)

Abstract: Charantins A is cucurbitane-type triterpene glycoside secondary metabolites derived from *Momordica charantia*. Here, biological activities of charantin A and mode of action to *Spodoptera litura* ovary cell line (SpLi-221) were evaluated. We investigated the effects of charantins A on cell growth inhibition compared with charantins B, momordicin I and azadirachtin A. Among them, charantins A showed the most potent activity against SpLi-221 cells with the lowest IC₅₀ values, and in a time- and dose-dependent manner. Moreover, the cell morphology changed after charantin A treatment, including cytoplasm leakage, irregular morphology, and apoptotic bodies. In addition, the flow cytometry assay confirmed that charantin A promoted the occurrence of cells' G2/M block and apoptosis, as evidenced by an increased ratio of cells in the sub-G1 phase. Furthermore, cell membrane disruption and increase of intracellular calcium levels were observed following charantin A treatment. These findings provide new clues regarding the role of cucurbitane-type triterpene glycosides as potential novel pesticides for pest control.

Keywords: *Momordica charantia*; tetracyclic triterpene; cytotoxicity; cell cycle; calcium homeostasis; *Spodoptera litura*. © 2018 ACG Publications. All rights reserved.

1. Introduction

The bitter melon, *Momordica charantia* L. (Cucurbitales: Cucurbitaceae) is widely used as a vegetable in Asia. A new cucurbitane-type tetracyclic triterpene, charantins A, were isolated from an

* Corresponding author: E-Mail: gzhbling@scau.edu.cn; Phone: +86 020 85283676 Fax: +86 020 85283676

† Equal contribution

dimethyl sulfoxide (DMSO), and Pluronic F-127 were purchased from Sigma-Aldrich, Missouri, US. Grace's insect culture medium and foetal bovine serum (FBS) were purchased from Invitrogen, California, US. The Cell Cycle Detection Kit was purchased from KeyGen BioTech Co. Ltd., Nanjing, China. Hank's Balanced Salt Solution (HBSS) was purchased from Solarbio Technology Co. Ltd., Beijing, China. Fluo 3-AM was purchased from Dojindo Molecular Technologies, Inc., Japan.

2.2. Cell Culture

The cell line TUAT-SpLi-221 (SpLi-221) originated from the culture of the pupal ovaries of *Spodoptera litura*. It was obtained from the State Key Laboratory of Biocontrol, Department of Biochemistry, School of Life Sciences, Sun Yat-sen University (Guangzhou, China). Cultures were maintained in 4 mL of Grace's insect culture medium supplemented with 10% foetal bovine serum, penicillin (100 µg/mL), and streptomycin (30 µg/mL) at 27 °C in a CO₂ incubator. Exponentially growing cells were used for the experiments.

2.3. Cell Viability Assay

Cell suspensions (5.0×10^4 cells/mL) were seeded in 96-well culture plates (100 µL/well). After a 24 h pre-incubation period, charantin A, charantin B, momordicin I and azadirachtin A were added to final concentrations of 2.5, 5, 10, 20 and 40 µg/mL, and 0.5% DMSO solution was used as the control (n = 10). After 24, 36, 48 and 60 h of treatment, 20 µL of MTT solution (5 mg/mL) was added to each well and incubated at 27 °C for 4 h. Next, the medium was discarded, and 100 µL of DMSO was added to dissolve the formazan crystals by shaking for 30 min in darkness. The absorbance was measured on a microplate reader (Bio-Rad, USA) at 490 nm. The cytotoxic effects were expressed as the relative percentage of inhibition and calculated as the following:

$$\text{Cell proliferation inhibition rate (\%)} = [(OD_{ck} - OD_{tr}) / OD_{ck}] \times 100$$

2.4. Inverted Phase Contrast Microscopy

SpLi-221 cells in the exponential growth phase were plated in a 6-well plate at a density of 1×10^5 cells/well. After 24 h of adherence growth, charantin A was added to a final concentration of 5 µg/mL. The morphological characteristics of SpLi-221 cells were recorded using an inverted phase contrast microscope (Olympus, Japan) after 24 and 48 h. Cells cultured with 0.5% DMSO were used as the control.

2.5. Flow Cytometric Analysis of the Cell Cycle and Apoptosis

SpLi-221 cells (1.0×10^7 cells/dish) were centrifuged and cultured for 12 h for cell cycle synchronisation by serum starvation. After treatment with 5 µg/mL charantin A for 24 and 48 h, cells were harvested and washed in PBS (pH = 7.2) twice and fixed in 70% ice-cold ethanol at 4 °C overnight. Prior to analysis, ethanol was removed by centrifugation (2000 rpm, 5 min), and the cells were washed and incubated in RNase A for 30 min at 37 °C. Next, the cells were stained with PI (50 µg/mL) solution in the dark for 30 min according to the instructions of the cell cycle detection kit prior to analysis using a FACSCalibur machine (Becton Dickinson, USA). A total of 20,000 cells were acquired in each assay. Analysis of cell cycle phase (G0/G1, S and G2/M) and the apoptosis rate were using Cell Quest and Modfit Software (Becton Dickinson) [16]. Each treatment was repeated four times, and cells cultured with 0.5% DMSO were used as the control.

2.6. Intracellular Free Ca²⁺ Analysis

Intracellular free calcium analysis was performed using a laser scanning confocal microscope (Leica 780, Germany). SpLi-221 cells (1.0×10^6 cells/dish) were centrifuged and treated with 5 µg/mL charantin A for 12 and 24 h. The supernatants were removed, and cells were rinsed three times in

HBSS (2000 rpm, 5 min). Fluorogenic Ca^{2+} indicator Fluo 3-AM (5 $\mu\text{mol/L}$) with a 0.05% final concentration of Pluronic F-127 was added to the incubated samples for 45 min at 37 °C. After dye loading, the cells were rinsed with HBSS at least three times. Coverslips of the labelled cells were mounted in 35-mm polystyrene tissue culture dishes (Corning, US) and incubated in HBSS for an additional 30 min at 37 °C prior to imaging. Fluo-3 fluorescence, which can be excited by an argon ion laser at 488 nm, was detected using LSCM. Ca^{2+} concentrations were expressed as the average fluorescence intensity of 50 cells/field, which were randomly selected from three fields in each treatment group of cells. Fluorescence data were analysed using Leica confocal software (ZEN 2012). Cells treated with 0.5% DMSO were used as the control.

2.7. Statistical Analysis

Analyses were performed using SPSS software version 19.0 (IBM Corporation). The cell toxicity regression equation and IC_{50} values were performed for the probit analysis. A repeated measures analysis of variance (ANOVA) was performed to evaluate the inhibition of cell proliferation during exposure to different concentrations of the investigated chemicals and exposure to different chemicals at the same concentrations, and the IC_{50} values were compared. Differences in the cycle distribution and calcium fluorescence intensity were compared using independent samples t-tests. A value of $p < 0.05$ was considered significant. All experiments were performed at least three times for each treatment dose group.

3. Results and Discussion

3.1. Charantin A Inhibited Cell Proliferation in *SpLi-221* Cells

Determination of cytotoxicity, a common method to evaluate the biological activities of natural products, is helpful to confirm whether plant extracts have potential pest-resistant properties [17]. To confirm the cytotoxic activities of the isolated compound, *SpLi-221* cells were treated with charantin A, charantin B, momordicin I and azadirachtin A for 24, 36, 48, and 60 h, and cell viability was assessed using the MTT assay (Table 1). Figure 2 illustrates cell growth inhibition directly correlates with presented concentrations of charantins A, suggesting a dose-dependent effect. Furthermore, the inhibitory effect seems to be time-dependent. Cell proliferation was nearly completely inhibited when cells were exposed to charantin A at 10 or 20 $\mu\text{g/mL}$ for 24 h. Overall, these results showed that charantins A exerted inhibitory activity on cellular growth, and the inhibitory effects of charantin A were more potent than momordicin I, charantin B and azadirachtin A. Thus, 5 $\mu\text{g/mL}$ charantin A was used in all further experiments.

Table 1. Anti-proliferative activity of tetracyclic triterpene compounds against the *SpLi-221* cell lines*

Treatment time (h)	Treatment	Toxicity regression equation	IC_{50} ($\mu\text{g/mL}$)	Correlation coefficient
24	Charantin A	$y=3.754+2.043x$	4.64a	0.897
	Charantin B	$y=2.456+2.545x$	9.51b	0.971
	Momordicin I	$y=3.914+1.663x$	5.16a	0.964
	Azadirachtin A	$y=3.186+0.936x$	29.51c	0.895
48	Charantin A	$y=5.380+0.835x$	2.41a	0.843
	Charantin B	$y=3.795+1.373x$	8.05c	0.952
	Momordicin I	$y=4.913+0.534x$	5.36b	0.803
	Azadirachtin A	$y=2.687+1.927x$	15.37d	0.973

Different lowercase letters following the data within column IC_{50} indicate a significant difference at $\alpha = 0.05$ level (Tukey's test, $p < 0.05$).

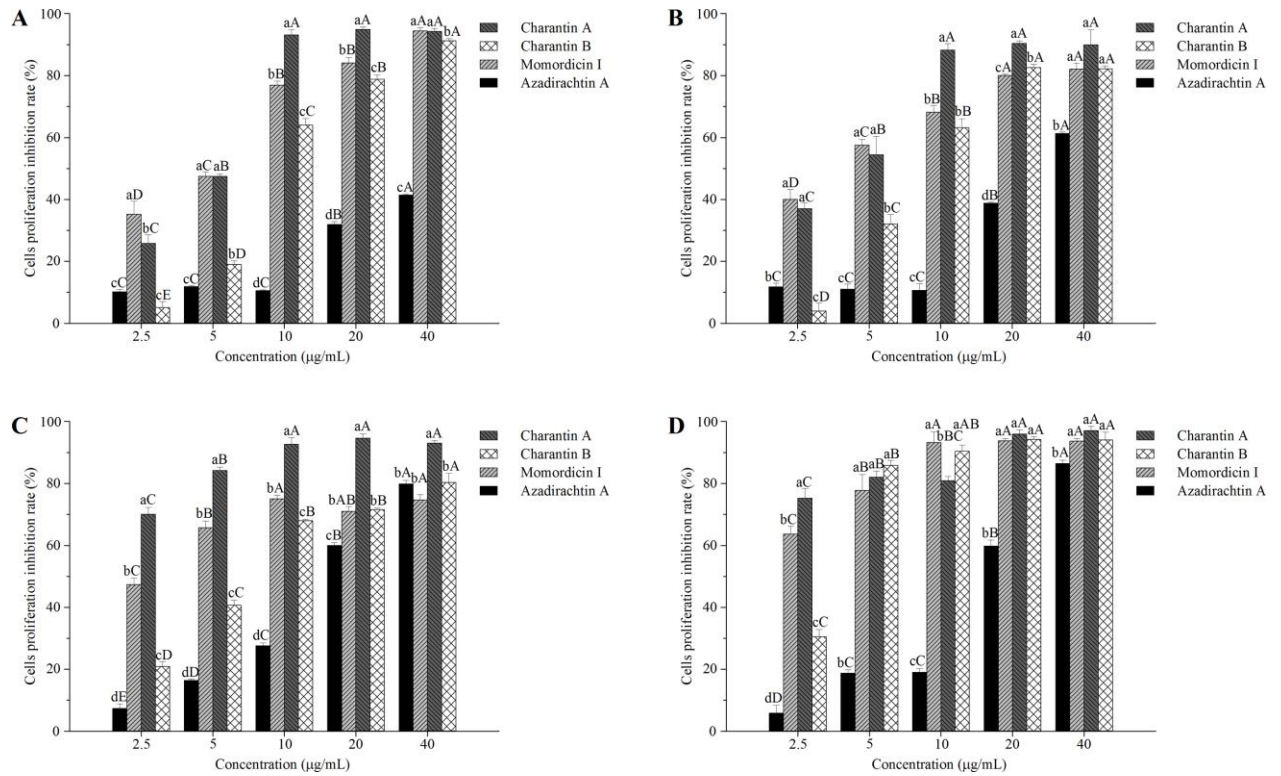


Figure 2. MTT assay analysis inhibitory effects of charantin A on SpLi-221 cell proliferation for 24 h (A), 36 h (B), 48 h (C), and 60 h (D). Values are expressed as the mean \pm SE of three independent experiments. Different capital letters indicate significant differences between the same chemical at different concentrations at the 0.05 level, and different lowercase letters indicate significant differences between different chemicals under the same concentration at the 0.05 level (Tukey's test, $p < 0.05$)

3.2. Morphological Effects of Charantin A on SpLi-221 Cells

With the exception of the cell viability assay, determining the morphological changes and characteristics of apoptosis are both useful methods to examine cytotoxicity. Cell morphology can directly reveal cell changes after exposure to a compound. So, inverted phase contrast microscopy was applied to assess morphological changes in SpLi-221 cells induced by 5 $\mu\text{g/mL}$ charantin A (Figure 3). Untreated control cells (Figure 3A, 3C) grew adhered to the culture plate while attached to each other forming a monolayer (arrow a). Control cells typically maintained a smooth surface, and normal size and morphology. On the other hand, after 24 h exposure to charantin A (Figure 3B), some cells were observed floating, and a corrugated surface (arrow b) and holes (arrow c) appeared. Intercellular space was clearly enlarged. After 48 h of exposure, cells showed obvious morphological changes, including cytoplasm shrinkage (arrow e) and leakage (arrow f), irregular morphology (arrow g), and apoptotic bodies with membrane blebbing (arrow d). In addition, cells failed to adhere and were observed resuspended in the culture medium (Figure 3D). These alterations were probably behind the toxic effects described above by MTT. Alteration of cell morphology was similar with SL-1 cell exposure to momordicins I and II [11], or azadirachtin A [14]. Apparently, charantin A can reduce SpLi-221 cell viability by destroying the morphological structure.

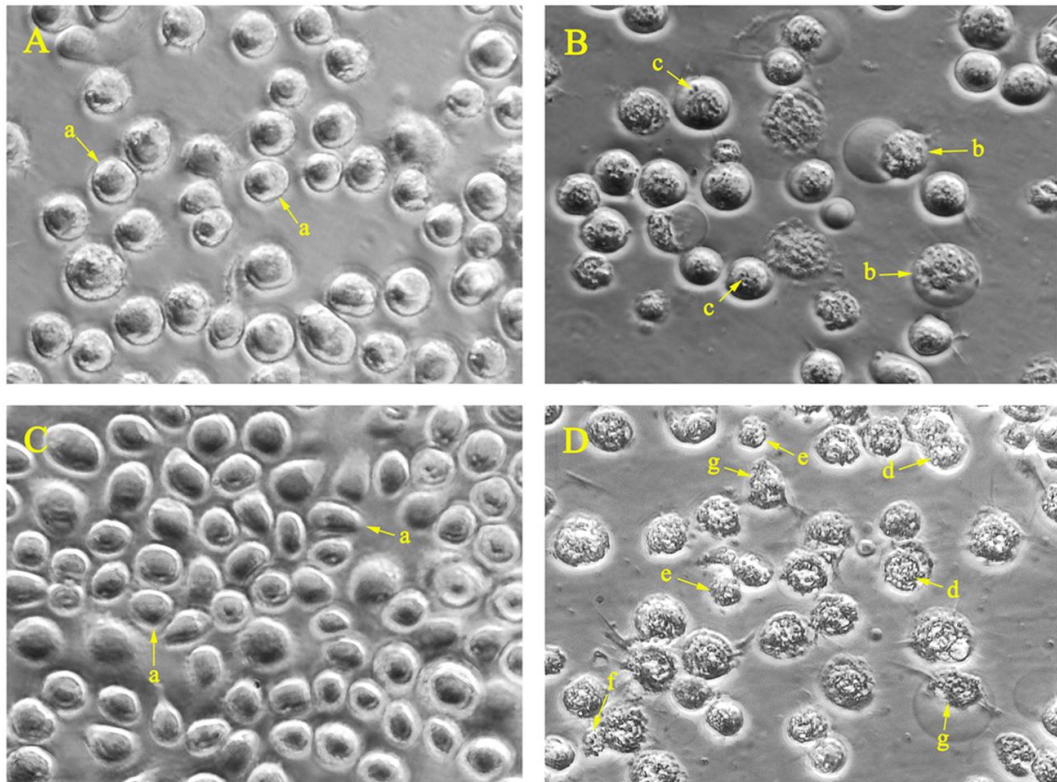


Figure 3. Observation of morphological changes of SpLi-221 cells treated with charantin A (5 $\mu\text{g/mL}$) using an inverted phase contrast microscope ($\times 200$). (A) and (C) are control cells in drug-free medium for 24 h and 48 h. (B) and (D) are cells treated with charantin A for 24 h and 48 h. (a-normal, b-rough surface, c- holes, d- apoptotic bodies, e-shrinkage, f-leaky cytoplasm, g-irregular)

3.3. Charantin A Induced Cell Cycle G2/M Arrest in SpLi-221 Cells

Cell proliferation is realized by the cell cycle, and regulation of the cell cycle is a complicated procedure. Cell cycle arrest is closely linked to cell proliferation [18,19]. The sensitivity of cell proliferation is often dependent on the cell cycle [20]. It was reported previously that some cytotoxic compounds directly induce apoptosis by arresting cells in cell phase cycles G0/G1, S, or G2/M prior to inducing apoptosis [14,21,22]. To determine if the inhibition of proliferation and morphological changes induced by charantin A in SpLi-221 cells are involved in cell cycle arrest, we examined the cell cycle phase distribution of the treated cells using flow cytometry. As a consequence, charantin A arrested SpLi-221 cells in the G2/M phase in a time-dependent manner and induced apoptosis, as suggested by an increase of cells at sub-G1 (Figure 4). Charantin A treatment resulted in accumulation of cells in the G2/M phase at 69.31% for 24 h of exposure to 75.80% at exposure for 48 h, with a proportional decrease in percentages at G0/G1 phase. These ratios were significantly different compared with DMSO-treated control cells (Table 2) (G2/M: $t_{24\text{h}} = -8.582$, $p < 0.01$; G0/G1: $t_{24\text{h}} = 9.073$, $p < 0.01$). After 48 h of exposure cells at G0/G1 had almost disappeared. Simultaneously, when cells were exposed to charantin A for 24 and 48 h, sub-G1 population increased from 0.91% to 2.64%, an increase of 8.27 and 12.57 fold relative to control cells, respectively. These findings were consistent with the results obtained with treatment with momordicin I and II in SL-1 cells [11]. Consistent with these findings, tetracyclic triterpenoids induced cell cycle arrest in the G2/M phase on insect cells.

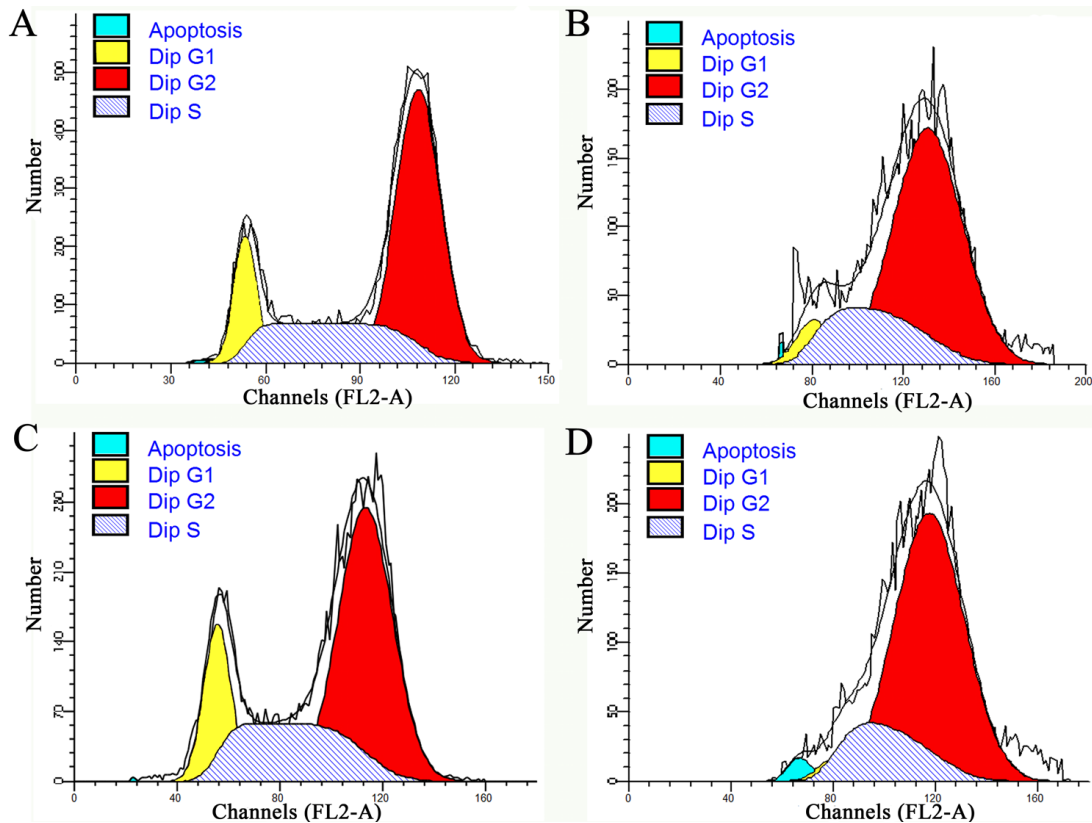


Figure 4. Flow cytometry analysis of the DNA content and apoptosis of SpLi-221 cells treated with charantin A. (A) and (C) were control cells in drug-free medium for 24 h and 48 h. (B) and (D) were cells treated with 5 µg/mL charantin A for 24 h and 48 h

Table 2. SpLi-221 cell cycle phase distribution analysis

Treatment	Cell cycle phase distribution (%)			
	sub-G1 (apoptosis)	G0/G1	S	G2/M
24 h Control	0.11±0.05	13.65±0.50	28.41±0.89	57.94±1.00
24 h Charantin A	0.91±0.18**	6.70±0.56**	24.00±0.70**	69.31±0.88**
48 h Control	0.21±0.06	16.09±0.14	27.36±0.32	56.55±0.20
48 h Charantin A	2.64±0.33*	0.14±0.07**	24.07±0.99	75.80±0.96**

Mean ± SE (n = 3) in the same row followed by * or ** are significantly different (*t*-test) for the same treatment time (**p* < 0.05, ***p* < 0.01 vs. control).

3.4. Charantin A Results in an Increase in Intracellular Free Ca^{2+} in SpLi-221 cells

Cell proliferation is critically dependent on the regulated movement of ions across various cellular compartments [23]. It is involved in many functions in proliferative cells, including gene expression, protein synthesis, cell secretion, metabolism, cell-cycle progression and apoptosis [24,25]. Numerous research studies have revealed that intracellular calcium homeostasis is a key factor for normal functions and structural integrity of the cell, such as cell proliferation, and the calcium concentration will quickly alter when the cells are stimulated [25-27]. As revealed by LSCM images, concentration of intracellular free calcium increased from exposure to charantin A. At increased exposure times, green fluorescence increased (Figure 5B, D). However, intracellular calcium seems to have remained stable throughout first 24h of exposure (Figure 5A, 5C). Moreover, Figure 5D shows

details within cells treated with charantin A for 24 h, which when comparing between cells in bright field (Figure 5E) with the merge field (Figure 5F), it seems evident control cells had smooth surface and regular shape, with distinct outlines shown by a slight fluorescence (arrow a). Exposed cells, on the other hand, were uneven and with unclear outlines amidst intense fluorescence (arrow b). Mean individual fluorescence (N = 450; Figure 5G) at 12h and 24h were significantly higher than negative controls 12 h and 24 h, respectively (** $p < 0.01$).

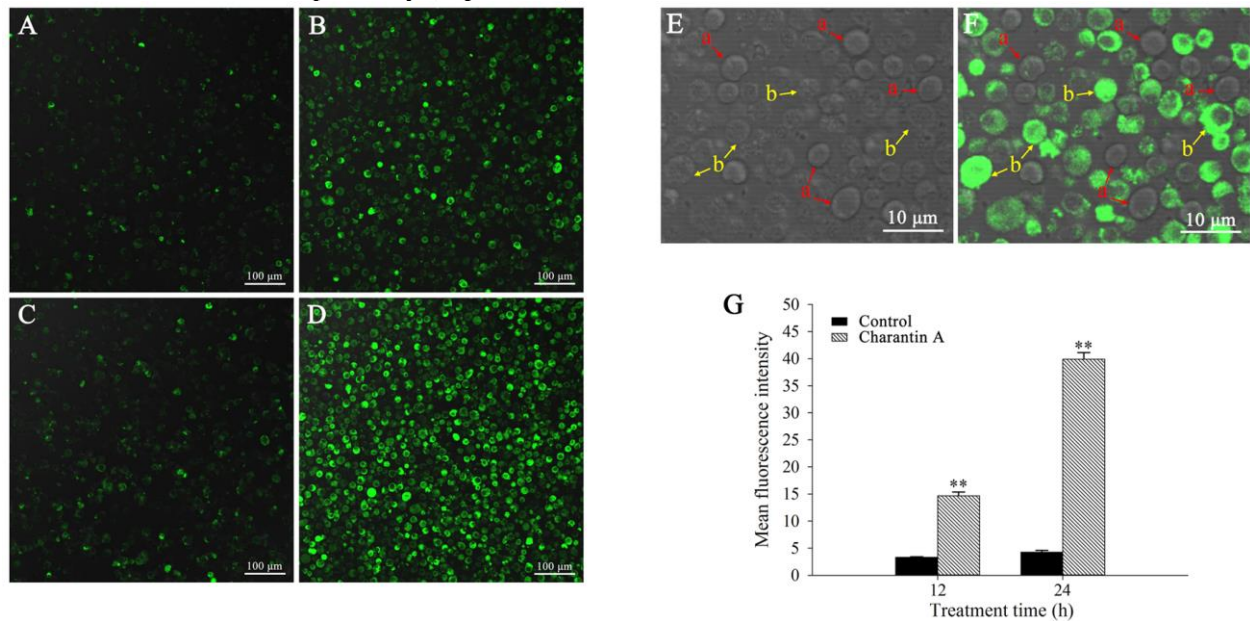


Figure 5. Intracellular-free Ca^{2+} changes analysis of SpLi-221 cells treated with charantin A by LSM. A-D: Fluorescence in dark field. E: bright field. F: merged field. (A) and (C) are control cells in drug-free medium for 12 h and 24 h. (B) and (D, E, F) are cells treated with 5 $\mu\text{g}/\text{mL}$ charantin A for 12 h and 24 h. Letter (a) represents normal or healthy cells, and (b) represents damaged cells. G: mean fluorescence intensity of SpLi-221 cells. Data are expressed as the mean \pm SE (n = 4) (** $p < 0.01$ vs. control)

4. Conclusions

In the present work we evaluated the biological activities of tetracyclic triterpene, charantins A, extracted from *M. charantia* leaves. Charantin A was exhibited potent cytotoxic activity against SpLi-221 cell lines, by inhibited cell proliferation with a time- and dose-dependent manner. Moreover, SpLi-221 cell was destroyed after charantin A treatment, including morphology changed, cell cycle arrested in G2/M phase and apoptosis occurred. The mechanism of action of charantin A with good cytotoxicity is unknown, but disruption of intracellular calcium homeostasis be suggested as a possible factor. The next work will focus on investigating the mechanism of action of these charantins. In a word, these findings provide new clues regarding the role of tetracyclic triterpene natural products as potential novel pesticides for pest control.

Acknowledgments

The authors thanks Eduardo Gonçalves Paterson Fox for helpful modification of manuscript, and thanks Dr. Yi Pang and Dr. Kai Yang from the State Key Laboratory of Biocontrol, Sun Yat-sen University, who kindly provided the insect cell lines.

Disclosure statement

The authors declare that they have no conflicts of interest.

Acknowledgement

This study was financially supported by the National Natural Science Foundation of China (No. 31171849).

ORCID

Zijun Guo: [0000-0002-7423-5430](https://orcid.org/0000-0002-7423-5430)

Guocai Wang: [0000-0002-4008-2640](https://orcid.org/0000-0002-4008-2640)

Maoxin Zhang: [0000-0002-8634-428X](https://orcid.org/0000-0002-8634-428X)

Guangwen Liang: [0000-0002-3018-7801](https://orcid.org/0000-0002-3018-7801)

Qiang Li: [0000-0001-5950-8843](https://orcid.org/0000-0001-5950-8843)

Bing Ling: [0000-0002-1572-3880](https://orcid.org/0000-0002-1572-3880)

References

- [1] Y.B. Zhang, H. Liu, C.Y. Zhu, M.X. Zhang, Y.L. Li, B. Ling and G.C. Wang (2014). Cucurbitane-type triterpenoids from the leaves of *Momordica charantia*, *J. Asian Nat. Prod. Res.* **16**, 358-363.
- [2] N. Beloin, M. Gbeassor, K. Akpagana, J. Hudson, K. De Soussa, K. Koumaglo and J. Arnason (2005). Ethnomedicinal uses of *Momordica charantia* (Cucurbitaceae) in Togo and relation to its phytochemistry and biological activity, *J. Ethnopharmacol.* **96**, 49-55.
- [3] J. Li, L.W. Zhang, E.Z. Yan and G.J. An (2005). The research progress on momordicoside, *Food Res. Dev.* **26**, 21-24.
- [4] M. Abe and K. Matsuda (2000). Feeding deterrents from *Momordica charantia* leaves to cucurbitaceous feeding beetle species, *Appl. Entomol. Zool.* **35**, 143-149.
- [5] X. Cao, C.Y. Zhu, M.X. Zhang and B. Ling (2015). Bioactivity of momordicin I against *Ostrinia furnacalis* (Lepidoptera: Pyralidae) and its effects on the metabolizing enzyme activities in larval bodies of the moth, *Acta Entomol. Sin.* **58**, 625-633.
- [6] B. Ling, G.C. Wang, Y.A. Ji, M.X. Zhang and G.W. Liang (2008). Antifeedant activity and active ingredients against *plutella xylostella* from *Momordica charantia* leaves, *Agric. Sci. Chin.* **7**, 1466-1473.
- [7] B. Ling, Y.L. Xiang, G.C. Wang, S.H. Chen and M.X. Zhang (2009). Antifeedant and antioviposition activities of *Momordica charantia* leaf ethanol extract against *Liriomyza sativae*, *Chin. J. Appl. Ecol.* **20**, 836-842.
- [8] D.B. Mekuria, T. Kashiwagi, S. Tebayashi and C.S. Kim (2005). Cucurbitane triterpenoid oviposition deterrent from *Momordica charantia* to the leafminer, *Liriomyza trifolii*, *Biosci. Biotech. Bioch.* **69**, 1706-1710.
- [9] H. Yasui, A. Kato and M. Yazawa (1998). Antifeedants to armyworms, *Spodoptera litura* and *Pseudaletia separata*, from bitter melon leaves, *Momordica charantia*, *J. Chem. Ecol.* **24**, 803-813.
- [10] Y. Luo, Z.J. Guo, G.C. Wang, X. Cao, M.X. Zhang and B. Ling (2013). Inhibitory effects of momordicin II on an experimental population of *Ostrinia furnacalis* (Güenée) and *Spodoptera litura* (Fabricius), *Int. Conf. Biol. Med. Chem. Eng.* **BMCE2013**, 221-227.
- [11] H. Liu, G.C. Wang, M.X. Zhang and B. Ling (2014). The cytotoxicology of momordicins I and II on *Spodoptera litura* cultured cell line SL-1, *Pestic. Biochem. Physiol.* **122**, 110-118.
- [12] H. Rembold and R.S. Annadurai (2014). Azadirachtin inhibits proliferation of Sf 9 cells in monolayer culture, *Z. Naturforsch. C.* **48**, 495-499.
- [13] A. Salehzadeh, A. Akhka, W. Cushley, R. Adams, J. Kusel and R. Strang (2003). The antimetabolic effect of the neem terpenoid azadirachtin on cultured insect cells, *Insect Biochem. Mol. Biol.* **33**, 681-689.
- [14] J.F. Huang, K.J. Shui, H.Y. Li, M.Y. Hu and G.H. Zhong (2011). Antiproliferative effect of azadirachtin A on *Spodoptera litura* SL-1 cell line through cell cycle arrest and apoptosis induced by up-regulation of p53, *Pestic. Biochem. Physiol.* **99**, 16-24.
- [15] J.F. Luo, H. Liu, Z.J. Guo, G.C. Wang and B. Ling (2016). Inhibition of cellular proliferation and induction of necrosis in Ofh cells of *Ostrinia furnacalis* (Lepidoptera: Pyralidae) by momordicin I and charantin B, *Acta Entomol. Sin.* **59**, 1093-1102.
- [16] X.Y. Huang, O.W. Li and H.H. Xu (2010). Induction of programmed death and cytoskeletal damage on *Trichoplusia ni* BTI-Tn-5B1-4 cells by azadirachtin, *Pestic. Biochem. Phys.* **98**, 289-295.

- [17] A. Itharat, P.J. Houghton, E. Eno-Amooquaye, P. Burke, J.H. Sampson and A. Raman (2004). *In vitro* cytotoxic activity of Thai medicinal plants used traditionally to treat cancer, *J. Ethnopharmacol.* **90**, 33-38.
- [18] Q.C. Liang, H. Xiong, Z.W. Zhao, D. Jia, W.X. Li, H.Z. Qin, J.P. Deng, L. Gao, H. Zhang and G.D. Gao (2009). Inhibition of transcription factor STAT5b suppresses proliferation, induces G1 cell cycle arrest and reduces tumor cell invasion in human glioblastoma multiforme cells, *Cancer Lett.* **273**, 164-171.
- [19] S.I. Okamoto, Y.J. Kang, C.W. Brechtel, E. Siviglia, R. Russo, A. Clemente, A. Harrop, S. McKercher, M. Kaul and S.A. Lipton (2007). HIV/gp120 decreases adult neural progenitor cell proliferation via checkpoint kinase-mediated cell-cycle withdrawal and G1 arrest, *Cell Stem Cell.* **1**, 230-236.
- [20] R.C. Taylor, S.P. Cullen and S.J. Martin (2008). Apoptosis: controlled demolition at the cellular level, *Nat. Rev. Mol. Cell Biol.* **9**, 231-241.
- [21] K. Matsumoto, Y. Akao, K. Ohguchi, T. Ito, T. Tanaka, M. Iinuma and Y. Nozawa (2005). Xanthenes induce cell-cycle arrest and apoptosis in human colon cancer DLD-1 cells, *Biorg. Med. Chem.* **13**, 6064-6069.
- [22] K. Torres and S. Horwitz (1998). Mechanisms of Taxol-induced cell death are concentration dependent, *Cancer Res.* **58**, 3620-3626.
- [23] L.R. Benzaquen, C. Brugnara, H.R. Byers, S. Gattoni-Celli and J.A. Halperin (1995). Clotrimazole inhibits cell proliferation *in vitro* and *in vivo*, *Nat. Med.* **1**, 534-540.
- [24] J.C. Sánchez and R.J. Wilkins (2004). Changes in intracellular calcium concentration in response to hypertonicity in bovine articular chondrocytes, *Comp. Biochem. Physiol. A: Mol. Integr. Physiol.* **137**, 173-182.
- [25] M.J. Berridge, P. Lipp and M.D. Bootman (2000). The versatility and universality of calcium signalling, *Nat. Rev. Mol. Cell Biol.* **1**, 11-21.
- [26] Y. Chen, S. Constantini, V. Trembovler, M. Weinstock and E. Shohami (1996). An experimental model of closed head injury in mice: pathophysiology, histopathology, and cognitive deficits, *J. Neurotrauma.* **13**, 557-568.
- [27] D.D. Limbrick Jr, S.B. Churn, S. Sombati, R.J. Delorenzo (1995). Inability to restore resting intracellular calcium levels as an early indicator of delayed neuronal cell death, *Brain Res.* **690**, 145-156.

ACG
publications

© 2018 ACG Publications